scientific reports

Check for updates

OPEN

# Population genetic structure and historical demography of *Saccostrea echinata* in the Northern South China sea and Beibu Gulf

Yafang Li[1,2,3], Lianggen Wang[1,2,3], Yingmin Wang[4], Quehui Tang[1,2,3], Shuangshuang Liu[1,2,3], Jiajia Ning[1,2,3], Delian Huang[1,2,3], Lei Xu[1,2,3]✉ & Feiyan Du[1,2,3]✉

**Marine invertebrates, such as oysters, were once thought to form large, panmictic populations with little genetic differentiation due to their high reproductive capacity and dual life stages. However, recent studies have shown significant genetic structuring and moderate gene flow across populations, influenced by factors like ocean currents, historical climate events, and environmental changes. The black-lip oyster (*Saccostrea echinata*), with its extensive dispersal potential, is ideal for population genetics studies. In current study, mitochondrial DNA (COI gene) was utilized to investigate the population structure, genetic diversity, and demographic history of *S. echinata* in the northern South China Sea (NSCS) and Beibu Gulf. Results revealed high genetic diversity with 82 haplotypes from 190 specimens, a star-shaped haplotype network, and significant genetic differentiation, with most variation occurring within populations. Genetic analysis identified three distinct genetic groups across the sampled regions. Historical demographic analysis indicated population expansion approximately 44–155 Kya after the Last Glacial Maximum. Genetic structure was shaped by historical climatic events causing isolation and secondary contact, as well as contemporary ocean currents influencing gene flow. The study highlights the complex interplay of genetic diversity, population structure, and historical dynamics in *S. echinata*, with implications for conservation and aquaculture in the Asia-Pacific region.**

**Keywords** Marine invertebrates, Genetic differentiation, Black-lip oyster (Saccostrea echinata), Mitochondrial DNA (COI gene), Population structure, Historical Climatic events

Marine invertebrates, especially oysters, are abundant in numbers, possess high reproductive capabilities, and exhibit a dual life history of both planktonic and sessile stages[1,2]. Traditionally, due to the strong dispersal potential of their larvae and the lack of substantial geographic barriers in the marine environment, it was believed that these species form a large, panmictic population, leading to genetic homogeneity even across large geographical scales. Consequently, these populations generally exhibit minimal genetic divergence and significant gene flow among individuals. However, research over the past 30 years has unveiled significant genetic differentiation among marine biological populations, revealing an overall genetic structure characterized by moderate spatial structuring coupled with pronounced gene flow[3–6]. Compared to terrestrial organisms, the factors influencing the genetic composition of marine organism communities are more complex. While these populations may exhibit a potential for high levels of gene flow, the actual rates of gene flow that exist are often much lower. Various factors-such as historical events, environmental selection, distance isolation, and rapid evolutionary processes can restrict gene flow among populations, even in the lack of apparent physical barriers[7,8]. Unique historical events significantly influence population divergence and speciation. Historical fluctuations in climate and environmental conditions can significantly impact the structure of marine biological populations, preserving information about these past climatic changes within their genetic framework[8,9]. Therefore, the genetic structure

[1]South China Sea Fisheries Research InstituteChinese Academy of Fishery Sciences, Guangzhou 510300, China. [2]Guangdong Provincial Key Laboratory of Fishery Ecology and Environment, Guangzhou 510300, China. [3]Sanya Tropical Fisheries Research Institute, Sanya, China. [4]James Cook University, Sims Dr 387380, Singapore, Singapore. ✉email: cloud_xu@hotmail.com; feiyanegg@163.com

of a species' population is probably shaped in the past and is often minimally influenced by contemporary gene flow.

At larger spatial scales, ocean currents can significantly influence the population genetic structure, particularly among adult sessile species[10]. Under the influence of ocean currents, dispersal between populations does not necessarily align with Euclidean spatial distances, subsequently affecting the isolation-by-distance pattern. Consequently, the positive relationship between genetic distance and spatial distance among populations may be weakened. Geographically distant populations could experience substantial gene flow due to the connectivity provided by certain current pathways, facilitating the dispersal of individuals over long distances. This connectivity enhances gene flow among populations situated along these current pathways, resulting in increased genetic diversity within populations and reduced differentiation between them, ultimately driving homogenization. Furthermore, ocean currents can create circulations and marine features, such as eddies and fronts, which can impede the passive dispersal of larvae, thereby serving as significant obstacles to gene flow between populations[11,12].

The *Saccostrea echinata* (Quoy and Gaimard, 1835), commonly known as the black-lip oyster, typically exhibits a round or elongated shape, characterized by fine growth lines resembling scales, with the edges curling into tube-like spines[13]. This species that live on rocky shores demonstrates good adaptability to varying temperatures and salinity and is broadly distributed throughout the Western and Southern Pacific Ocean[14]. Due to its low capital requirements, straightforward aquaculture techniques, and the stability of its hatchery culture, it is regarded as a promising candidate for marine aquaculture in the tropical regions of the Asia-Pacific[14,15]. This capability holds significant potential to promote the development and expansion of the oyster aquaculture industry across tropical regions of Australia and the Asia-Pacific region[14–16]. Moreover, its high reproductive capacity, substantial spawning output, strong dispersal capabilities, and extended larval planktonic phase make *S. echinata* an ideal subject for studying population genetic diversity, genetic structure, and historical dynamics against the backdrop of changing ocean currents. This study was designed to assess the distribution of haplotypes, genetic architecture, demographic history, and estimate the expansion timeline of *S. echinata* in the northern South China Sea, utilizing a segment of the mitochondrial cytochrome c oxidase subunit I (COI) gene as the molecular marker. Furthermore, it aims to provide reliable data to support the large-scale cultivation of *S. echinata*.

## Results

### Genetic diversity

Following alignment, 190 high-quality COI sequences from *S. echinata* were retrieved, with each sequence measuring 613 base pairs. The mean base composition consisted of 23.76% adenine (A), 16.47% cytosine (C), 19.47% guanine (G), and 40.3% thymine (T). These analysis uncovered a notably high level of genetic diversity in *S. echinata*, with 190 sequences resulting in 82 distinct haplotypes. The nucleotide diversity averaged 0.00829, spanning a range from 0.00446 to 0.01011, and haplotype diversity was 0.896 (ranging from 0.614 to 0.960) (Table 1).

The haplotype network of *S. echinata* from the northern South China Sea (NSCS) and the Beibu Gulf displayed a star-like configuration, characterized by a central haplotype (H5) that occurred at a high frequency (26.3%). The most frequent haplotypes are distributed across 9 out of the 11 sampling sites. Another haplotype (H18) also occurred at an elevated frequency (18.4%), was exclusively distributed in Daya Bay and Pearl River Estuary. All haplotypes of *S. echinata* from the northern South China Sea (NSCS) and the Beibu Gulf likely originated from a single ancestral haplotype (Fig. 2). In current study, the 82 haplotype sequences identified have been uploaded in GenBank and are accessible via accession numbers PQ782955 to PQ783036. Of the 82 haplotypes identified, 69 were restricted to specific sampling locations, whereas 13 were distributed across various locations. Notably,

| Sampling sites | *N* | H | S | Hd | π |
|---|---|---|---|---|---|
| S1 | 13 | 6 | 13 | 0.641 ± 0.022 | 0.00577 ± 0.00153 |
| S2 | 21 | 10 | 24 | 0.776 ± 0.093 | 0.00834 ± 0.00144 |
| S3 | 17 | 10 | 19 | 0.838 ± 0.087 | 0.00758 ± 0.00088 |
| S4 | 17 | 10 | 24 | 0.794 ± 0.103 | 0.00801 ± 0.00147 |
| S5 | 20 | 12 | 25 | 0.811 ± 0.092 | 0.00804 ± 0.00131 |
| S6 | 19 | 11 | 32 | 0.830 ± 0.085 | 0.00950 ± 0.00160 |
| S7 | 13 | 8 | 20 | 0.808 ± 0.113 | 0.00732 ± 0.00155 |
| S8 | 19 | 8 | 14 | 0.614 ± 0.130 | 0.00446 ± 0.00130 |
| S9 | 24 | 17 | 27 | 0.960 ± 0.025 | 0.00958 ± 0.00084 |
| S10 | 17 | 8 | 12 | 0.779 ± 0.099 | 0.00482 ± 0.00097 |
| S11 | 10 | 8 | 24 | 0.933 ± 0.077 | 0.01011 ± 0.00197 |
| Overall | 190 | 82 | 77 | 0.896 ± 0.017 | 0.00829 ± 0.00044 |

**Table 1**. Measures of genetic diversity of *Saccostrea echinata* from the Northern South China sea and the Beibu Gulf through descriptive statistics using COI sequence data. The geographical locations corresponding to the sampling sites listed in the table can be found in Fig. 1. *N* sample size, *H* number of haplotypes, *S* number of polymorphic sites, *Hd* haplotype diversity (± S.D.), *π* nucleotide diversity (± S.D.).

| Source of variation | d.f. | Sum of squares | Variance components | Percentage of variation | *p* |
|---|---|---|---|---|---|
| Among groups | 4 | 47.125 | 0.253 | 9.75 | < 0.005 |
| Among population within groups | 6 | 14.442 | 0.004 | 0.15 | < 0.005 |
| Within populations | 179 | 418.717 | 2.339 | 90.1 | < 0.005 |
| Total | 189 | 480.284 | 2.596 | | |

**Table 2**. Results of the analysis of molecular variance (AMOVA), partitioning overall mitochondrial DNA ($\Phi_{ST}$, using an infinite allele model) within and among groups.

| | S1 | S2 | S3 | S4 | S5 | S6 | S7 | S8 | S9 | S10 | S11 |
|---|---|---|---|---|---|---|---|---|---|---|---|
| S1 | 0 | | | | | | | | | | |
| S2 | −0.03054 | 0 | | | | | | | | | |
| S3 | **0.1942** | **0.16281** | 0 | | | | | | | | |
| S4 | **0.15436** | **0.13081** | −0.00236 | 0 | | | | | | | |
| S5 | −0.04305 | −0.01088 | **0.14291** | **0.11878** | 0 | | | | | | |
| S6 | −0.02055 | −0.01663 | **0.18155** | **0.13206** | −0.01706 | 0 | | | | | |
| S7 | **0.16585** | **0.1344** | 0.00622 | −0.0413 | **0.122** | **0.13181** | 0 | | | | |
| S8 | **0.23305** | **0.19041** | **0.10411** | −0.00497 | **0.17843** | **0.17051** | −0.01402 | 0 | | | |
| S9 | **0.15364** | **0.13469** | −0.0204 | −0.01768 | **0.11505** | **0.13593** | −0.00988 | **0.05866** | 0 | | |
| S10 | **0.21894** | **0.18155** | 0.04467 | −0.01145 | **0.17328** | **0.18817** | −0.03271 | −0.00675 | 0.03888 | 0 | |
| S11 | **0.16037** | **0.12342** | **0.05211** | −0.0256 | **0.11401** | **0.08604** | −0.02876 | −0.00796 | −0.00985 | 0.03385 | 0 |

**Table 3**. Pairwise differentiation $\Phi_{ST}$ of *Saccostrea echinata* sampled from Northern South China sea and the Beibu Gulf based on COI sequence data. Bold indicates significant pairwise $\Phi_{ST}$.

two of the more prevalent haplotypes were detected across multiple locations, indicating a broader distribution range distribution. This haplotype was detected at S2 and S11, which are more than 780 km apart. The site with the highest number of haplotypes is S9, with 17 haplotypes, while the lowest is S1, with 6 distinct haplotypes. Notably, site S11 produced 8 distinct haplotypes from just 10 specimens.

The results of AMOVA indicated that there was a significant difference in genetic structure between the northern South China Sea (NSCS) and the Beibu Gulf. Approximately 9.75% of the overall mitochondrial DNA genetic variation stems from five distinct sampling regions: Daya Bay (S1, S2), Pearl River Estuary (S3, S4), Huangmaohai Bay (S5, S6), the eastern regions of Leizhou Peninsula (S7, S11), and the Beibu Gulf (S8, S9, S10). In other words, the *S. echinata* populations in the NSCS exhibit significant genetic structuring, albeit small in scale. A significant portion (90.1%) of the overall genetic variance was attributed to differences occurring within populations. (Table 2). The mean genetic differentiation $\Phi_{ST}$ of *S. echinata* within the NSCS and the Beibu Gulf was 0.133 ranging from − 0.043 to 0.233. Additionally, *S. echinata* showed significant pairwise $\Phi_{ST}$ values among the five different sampling regions, Daya Bay (S1, S2), Pearl River Estuary (S3, S4), Huangmaohai Bay (S5, S6), eastern regions of Leizhou Peninsula (S7, S11), and Beibu Gulf (S8, S9, S10) (Table 3). PCoA analysis indicated that the genetic structure of the population was spatially divided into three distinct groups (Fig. 3). The first dimension accounted for 32% of the total variance, whereas the second dimension accounted for 20%. The number of effective migrants per generation between the five regions was shown in Fig. 4. The highest number of effective migrants per generation was observed from the Huangmaohai Bay population (S5, S6) toward the eastern Leizhou Peninsula population (S7, S11), reaching 47.3. The lowest number of effective migrants per generation was observed from the Beibu Gulf (S8, S9, S10) toward the Daya Bay population (S1, S2), only 0.62. (see Supplementary table).

## Historical demography

For *S. echinata* in the northern South China Sea (NSCS) and Beibu Gulf, both Tajima's D and Fu's Fs values exhibited statistically significant negative results (Tajima's D = −1.013, $p < 0.05$; Fu's Fs =−1.75, $p < 0.05$) (Table 4). These significant negative results indicate that the population may have undergone recent expansion, leading to an accumulation of low-frequency variants. The non-significant Raggedness Index and SSD also indicate that the actual data fit well with the population expansion model, showing no significant deviation from expected patterns (Table 4). The mismatch distribution displayed a bimodal distribution pattern (Fig. 5), which indicates that the *S. echinata* population had undergone historical isolation and secondary contact, possibly due to geographic or environmental barriers, followed by re-mixing due to environmental changes or migration. In the context of the historical demographic analysis, all samples were integrated, resulting in a τ value of 7.606 (95% confidence interval: 2.167–22.803). Considering that mitochondrial genes in oysters mutate at a rate of 2% within each million-year timeframe, the estimated expansion period for *S. echinata* in the NSCS and Beibu Gulf is believed to be between 44 and 155 thousand years ago. According to the Bayesian skyline plot (BSP) analysis, the haplotypes of *S. echinata* in this study converged around 200 Kya, assuming a mitochondrial gene mutation

| sites | Tajima's D | | Fu's Fs | | Mismatch distribution | | | | |
|---|---|---|---|---|---|---|---|---|---|
| | D | *p* | Fs | *p* | τ (95% CI) | SSD | SSD *p* | *R* index | *R* index *p* |
| S1 | −0.639 | 0.297 | 0.34 | 0.593 | 7.828 (0.377, 60.828) | 0.07856 | 0.2 | 0.16963 | 0.22 |
| S2 | −0.89 | 0.184 | −0.613 | 0.097 | 8.252 (2.479, 12.611) | 0.06982 | 0.04 | 0.11676 | 0.06 |
| S3 | −0.682 | 0.268 | −1.769 | 0.017 | 6.449 (1.705, 8.904) | 0.04146 | 0.1 | 0.07721 | 0.18 |
| S4 | −1.237 | 0.04 | −1.578 | 0.007 | 8.08 (2.805, 10.914) | 0.04762 | 0.15 | 0.12684 | 0.05 |
| S5 | −1.162 | 0.028 | −2.732 | 0.102 | 7.818 (2.584, 10.957) | 0.04852 | 0.13 | 0.07812 | 0.23 |
| S6 | −1.449 | 0.029 | −1.397 | 0.026 | 8.232 (2.439, 10.979) | 0.03966 | 0.1 | 0.04949 | 0.23 |
| S7 | −1.299 | 0.015 | −1.015 | 0.269 | 7.479 (1.457, 10.551) | 0.04579 | 0.24 | 0.09024 | 0.29 |
| S8 | −1.175 | 0.141 | −1.278 | 0.024 | 7.303 (0.299, 93.303) | 0.05282 | 0.41 | 0.12674 | 0.55 |
| S9 | −0.704 | 0.279 | −6.438 | 0.006 | 7.375 (4.312, 9.414) | 0.01105 | 0.28 | 0.02115 | 0.5 |
| S10 | −0.627 | 0.067 | −1.346 | 0.052 | 6.689 (0.453, 10.432) | 0.02223 | 0.58 | 0.04163 | 0.83 |
| S11 | −1.279 | 0.132 | −1.425 | 0.161 | 8.156 (4.926, 11.938) | 0.06576 | 0.06 | 0.15358 | 0.05 |
| total | −1.013 | 0.0463 | −1.75 | 0.015 | 7.606 (2.167, 22.803) | 0.04757 | 0.20818 | 0.09558 | 0.29 |

**Table 4**. Mismatch distribution, Tajima's D and Fu's Fs statistics for *Saccostrea echinata*.

rate of 2% p within each million-year timeframe[17]. Moreover, a sustained population expansion was observed between 30 and 50 Kya (Fig. 6).

The geographical locations corresponding to the sampling sites listed in the table can be found in Fig. 1.*SSD* sum of squared deviation, *R index* Raggedness index.

## Discussion

Mitochondrial DNA, due to its maternal inheritance, high mutation rate, and simple genome structure, has become a widely used tool in phylogenetic construction, population genetics studies, particularly for analyzing population history, migration patterns, and genetic diversity[18–20]. In our study, mitochondrial DNA was utilized to explore the population genetic structure of *S. echinata*, revealing high haplotype diversity, significant population structure differentiation, and complex dispersal and population history dynamics. Genetic diversity constitutes a fundamental pillar in facilitating a species' ability to thrive and adapt in response to environmental transformations, combat diseases, and propel evolution. It enhances population adaptability and survival, reduces the risk of inbreeding depression, and helps maintain ecosystem stability and functionality, which are critical for the species' long-term survival and evolution[21–23]. In our case, 190 specimens yield 82 haplotypes. The genetic diversity of *S. echinata* is characterized by high haplotype and nucleotide diversity, with an average nucleotide diversity of 0.00829 (> 0.005) and haplotype diversity of 0.896 (> 0.5)[24]. These values exceed those reported in other oyster and bivalve species. For instance, *Crassostrea gigas* and *Crassostrea sikamea* with haplotype diversity values of 0.423 and 0.730, respectively, and nucleotide diversity values of 0.002 and 0.004[25]. Similarly, the Japanese scallop exhibits haplotype diversity of 0.817 and nucleotide diversity of 0.008[26]. Sites with relatively high haplotype diversity were located in Huangmaohai Bay (S5 and S6), Beibu Gulf (S9), and the eastern Leizhou Peninsula (particularly in southeastern region of Hainan Island, S11). Usually, high haplotype diversity within oyster population or other sessile organisms are often attributed to a combination of factors. These include a large effective population size, which facilitates the retention of genetic variation, and the high mutation rate of mitochondrial DNA, which generates new haplotypes over time. Additionally, the admixture of populations from distinct origins further enhances genetic variation, leading to higher haplotype diversity (0.546–0.996)[25–27]. The genetic diversity level of *S. echinata* regarding COI polymorphisms was consistent with similar bivalves' study[28,29]. Other studies have reported a genetic diversity pattern in co-distributed oysters, characterized by some populations exhibiting high haplotype diversity (H, 0.737–0.996) but low nucleotide diversity (π, 0.001–0.004)[25], and others displaying both high haplotype diversity (H, 0.546 -1.000) and high nucleotide diversity (π, 0.005–0.009)[30]. These studies speculated that this pattern may result from contemporary evolutionary forces, such as gene infiltration caused by the introduction of different strains, habitat discontinuity, and population instability[25,30].

In our study, both the AMOVA and PCoA analysis indicated a relatively clear genetic differentiation of *S. echinata* between the habitats in the northern South China Sea (NSCS) and the Beibu Gulf (Table 2; Fig. 3). The genetic structure of population was spatially separated into three groups. The populations at the S1 and S2 sites in Daya Bay had similar genetic structure. S3, S4 in Pearl River Estuary and S5, S6 in Huangmaohai Bay had similar population's genetic structure. Previous research had demonstrated that the population genetic structure of bivalves typically exhibits high genetic diversity and considerable population differentiation[28]. First, bivalves generally show high haplotype diversity (H), particularly in species with wide distributions or strong adaptability. This is mainly attributed to their high reproductive capacity and the substantially elevated mutation rate evident in mitochondrial DNA (See the discussion above). Although *S. echinata* has a prolonged planktonic larval phase, spawning during the rainy season (summer) aligns with monsoon-driven currents. Localities outside these dominant dispersal corridors (e.g., Beibu Gulf) receive fewer migrants, leading to isolation. Larval retention mechanisms or settlement preferences in specific microhabitats could further limit gene flow. Second, the genetic structure of bivalve populations is influenced by geographic isolation and gene flow. In areas with connected habitats or coastal regions, genetic differentiation between populations is usually low. In contrast,

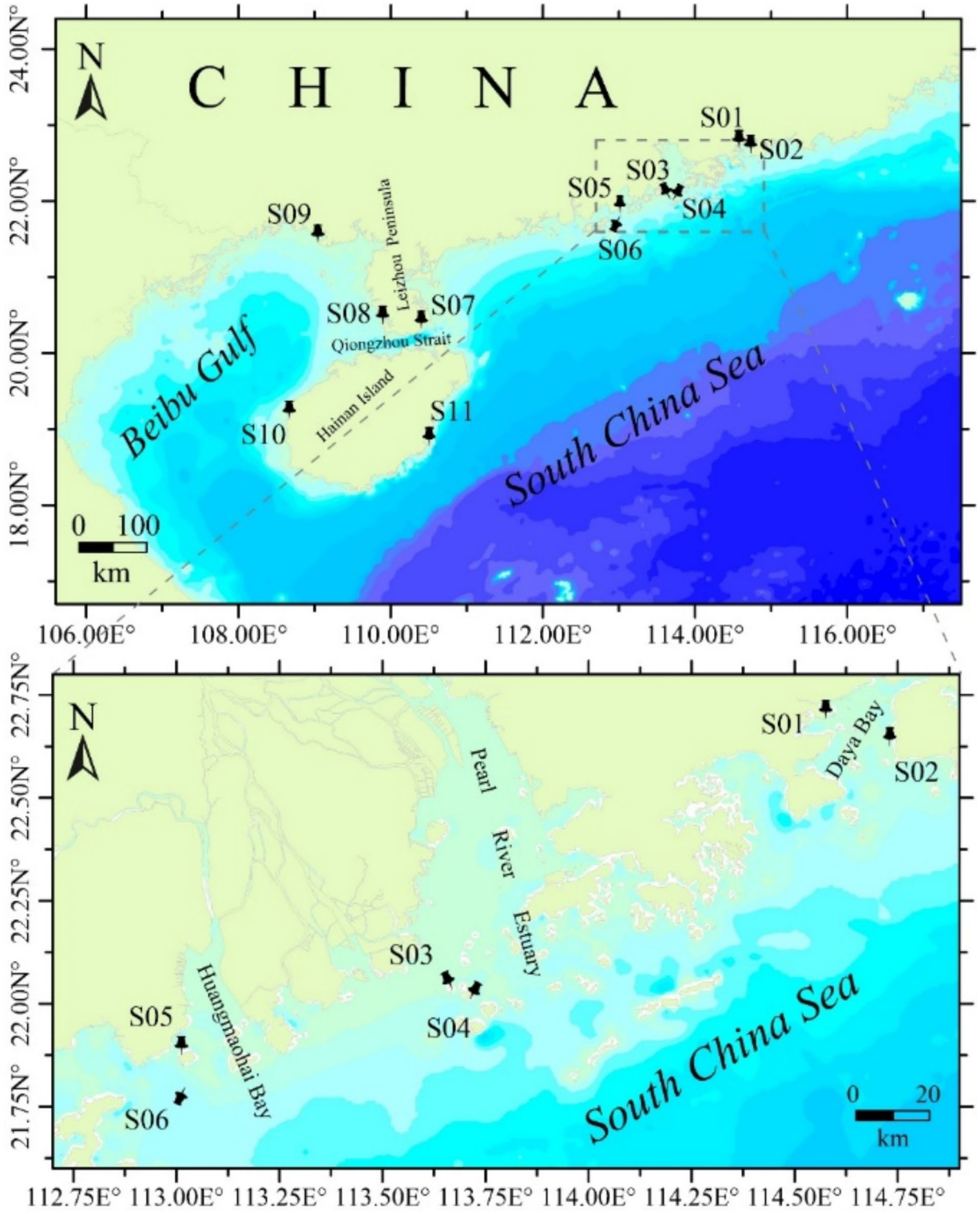


**Fig. 1**. A map illustrating the study region with 11 sampling locations in the northern South China Sea and the Beibu Gulf. This map was created using QGIS software, version 3.34.4-Prizren, which can be downloaded at https://qgis.org.

regions with geographic barriers or environmental gradients, such as variations in salinity or temperature, often demonstrate a pronounced and significant genetic divergence[25,31]. The Beibu Gulf's isolation is exacerbated by its distinct marine environment, which differs in salinity, temperature, and sediment composition from NSCS habitats. These environmental gradients may act as ecological barriers, reducing the survival or settlement of dispersing larvae even if some physical exchange occurs. Similarly, Daya Bay's unique hydrographic conditions

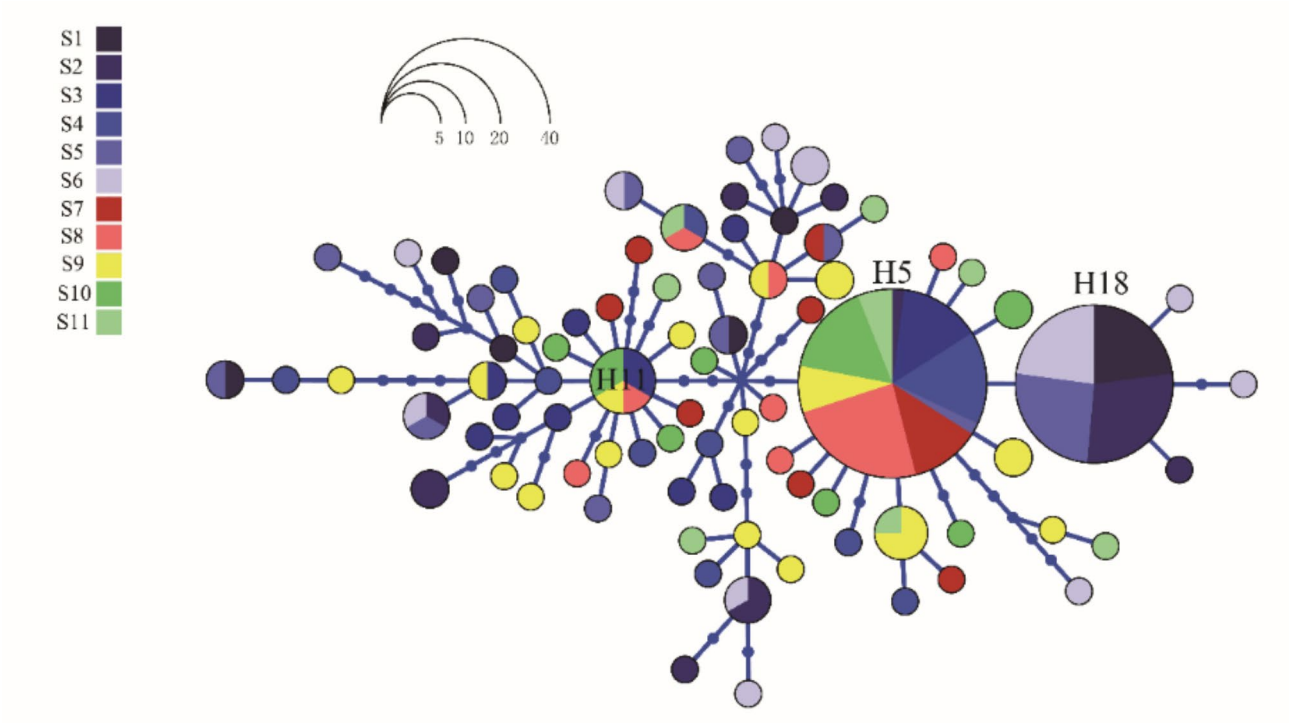


**Fig. 2**. A haplotype network was constructed for *Saccostrea echinata* based on genetic differences found in the nucleotides of the cytochrome c oxidase subunit I (COI) gene. The size of each circle denotes the frequency of individuals sharing a specific haplotype, with every circle representing a unique genetic variation. Each small dot on the haplotype branch represents a single mutation.

(e.g., lower salinity influenced by freshwater input) may create a localized adaptive environment, further differentiating its populations from others. As a result, the highest pairwise differentiation ($\Phi_{ST}$) was observed between S1 (Daya Bay) and S8 (Beibu Gulf). Third, bivalves typically undergo reproductive dispersal during their larval stage, which facilitates gene flow. However, factors including ocean currents, habitat fragmentation, and environmental variability may limit gene exchange, leading to the formation of regional genetic structures[31,32]. The highest effective number of migrants per generation was observed from the Huangmaohai Bay population (S5, S6) toward the eastern Leizhou Peninsula population (S7, S11), reaching 47.3. This indicates that there is significant dispersal between these two regions. The basic biology of *S. echinata* indicated that its breeding season was concentrated during the rainy season (summer), with high reproductive capacity, and its larvae had a longer planktonic period and stronger dispersal ability[33]. In the summer (from May to October), the sea currents between Huangmaohai Bay, the Pearl River Estuary, and the western Leizhou Peninsula are primarily influenced by the southeast monsoon, with the currents generally flowing from south to north. Water flows from the South China Sea toward the Pearl River Estuary, passes through Huangmaohai Bay, enters the western Guangdong region, and continues flowing northward, ultimately affecting the western Leizhou Peninsula. These coastal currents may carry the planktonic larvae of *S. echinata*, facilitating long-distance dispersal[20,34]. The last, historical events such as climate changes and sea level fluctuations have had a profound effect on the genetic structure of bivalve populations. Ice ages or climatic shifts may cause population bottlenecks or expansions, affecting the distribution of genetic diversity and genetic differentiation patterns. This issue is inherently complex and warrants a more thorough examination.

As sessile organisms inhabiting coastal zones, oysters are highly sensitive to changes in the coastal environment, which directly influence their distribution range. Climatic fluctuations during glacial and interglacial periods, accompanied by significant sea-level changes, have profoundly shaped coastal habitats. Sea-level drops can lead to the isolation of populations, while subsequent rises enable habitat expansion and promote secondary contact or mixing among previously separated populations[25,30]. The northern South China Sea (NSCS) and the Beibu Gulf have undergone substantial modifications due to the Pleistocene glacial and interglacial cycles, especially during the period of the Last Glacial Maximum (LGM), which transpired around 20 millennia ago, representing a pivotal moment in Earth's geological history. During glacial periods, much of the northern South China Sea (NSCS) shelf was exposed, and the Beibu Gulf was integrated into the South China mainland, becoming an essential component thereof. Prior to subsequent geological transformations that significantly altered the regional landscape, Hainan Island was integrally connected to the extensive mainland of China[35]. Based on the genetic patterns observed in our data, we inferred that the population of *S. echinata* likely underwent an expansion subsequent to the last glacial maximum (LGM). The estimated timing of this expansion ranges from approximately 44 to 155 Kya, potentially occurring during the last interglacial maximum around 115 Kya and continuing into the post-LGM period. It is worth noting that the mismatch distribution displayed a dual-peak

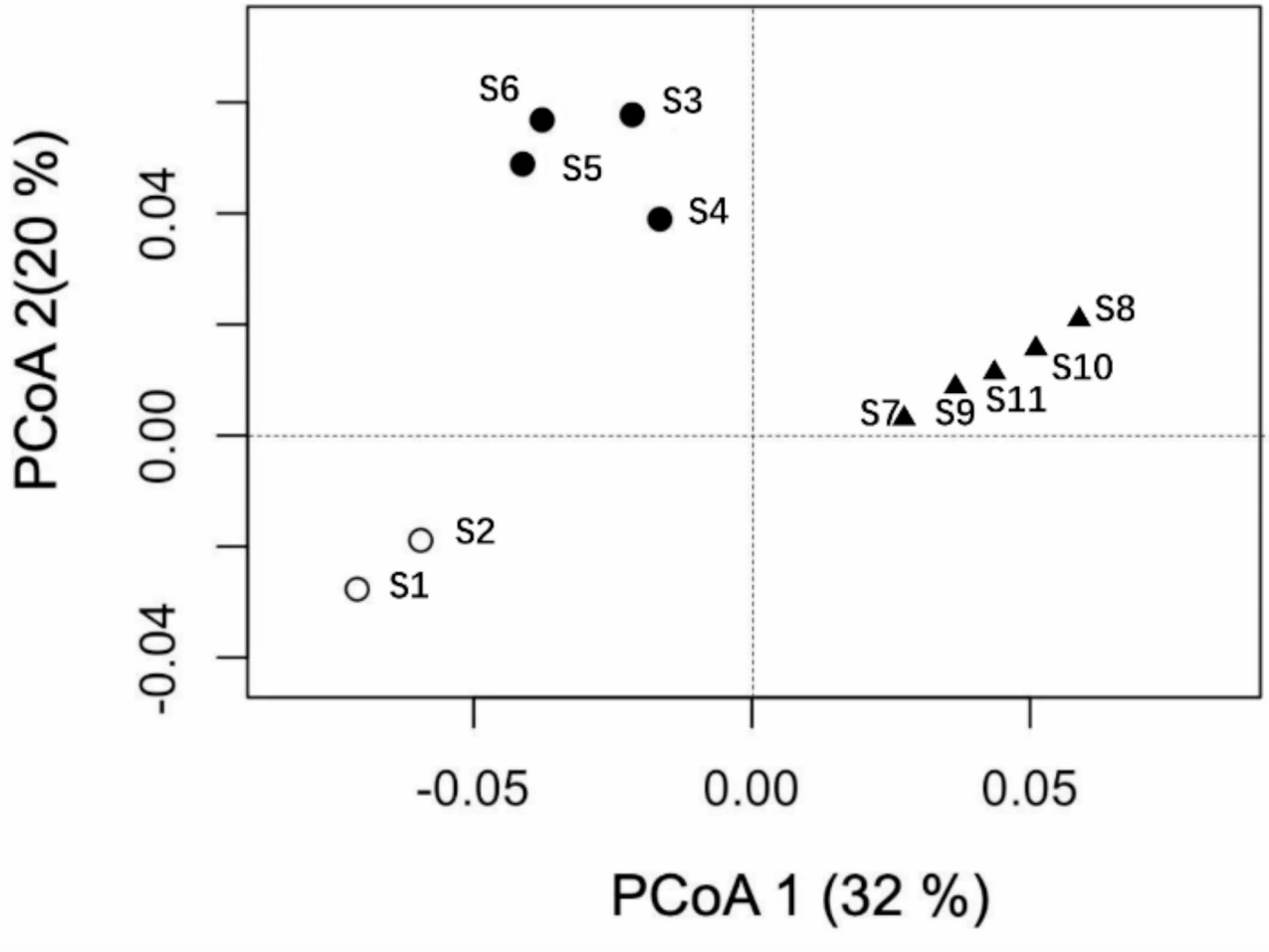


**Fig. 3**. Biplot of principle coordination analysis showing the linearized pairwise $\Phi_{ST}$. Solid circles represent the sampling locations in the Pearl River Estuary and Huangmaohai Bay, open circle represents the sampling locations in Daya Bay, and solid triangles represent the sampling locations in eastern Leizhou Peninsula and Beibu Gulf.

pattern (Fig. 5), suggesting that the *S. echinata* population experienced historical isolation, followed by secondary contact and re-colonization. During the last glacial maximum, lower sea levels likely caused geographic isolation of populations, promoting genetic differentiation as they evolved independently. As the climate warmed and sea levels rose in the post-LGM period, these isolated populations may have reunited, facilitating gene flow and the mixing of previously separated genetic lineages. The bimodal distribution reflected this process, with one peak representing the initial isolation and the other indicating the subsequent re-expansion and admixture of populations. Similar patterns have been observed and confirmed in other marine regions as well. For instance, Reeb and Avise[36]discovered a significant genetic structure along the eastern coastline of Florida, despite the absence of clear isolation barriers, with mitochondrial DNA differences reaching 3%. This genetic differentiation was attributed to the glacial periods when lowered sea levels caused coastal estuaries to dry up, leading to population isolation. Similarly, research on the Gulf of Mexico stone crab showed that eastern and western populations became isolated during the Pliocene and Pleistocene due to sea-level fluctuations, which resulted in allopatric speciation. Today, these two species are widely distributed across the southeastern United States, with a broad hybrid zone forming along the Gulf of Mexico[37]. During the Pleistocene, significant changes occurred in the marine fauna of the tropical Pacific region. While sea surface temperatures remained relatively stable during the ice ages, sea levels fluctuated by over 150 m[38]. These fluctuating sea levels, combined with the formation and disappearance of coral reefs and islands, caused marine species dependent on island habitats to repeatedly experience local extinction and re-colonization. This process has shaped the current species composition and population genetic structure[39,40].

## Materials and methods

### Study area

The South China Sea (SCS), situated in the northwestern Pacific Ocean, is the largest semi-enclosed sea in the tropical and subtropical regions, covering an area of approximately 3.3 million square kilometers. The northern

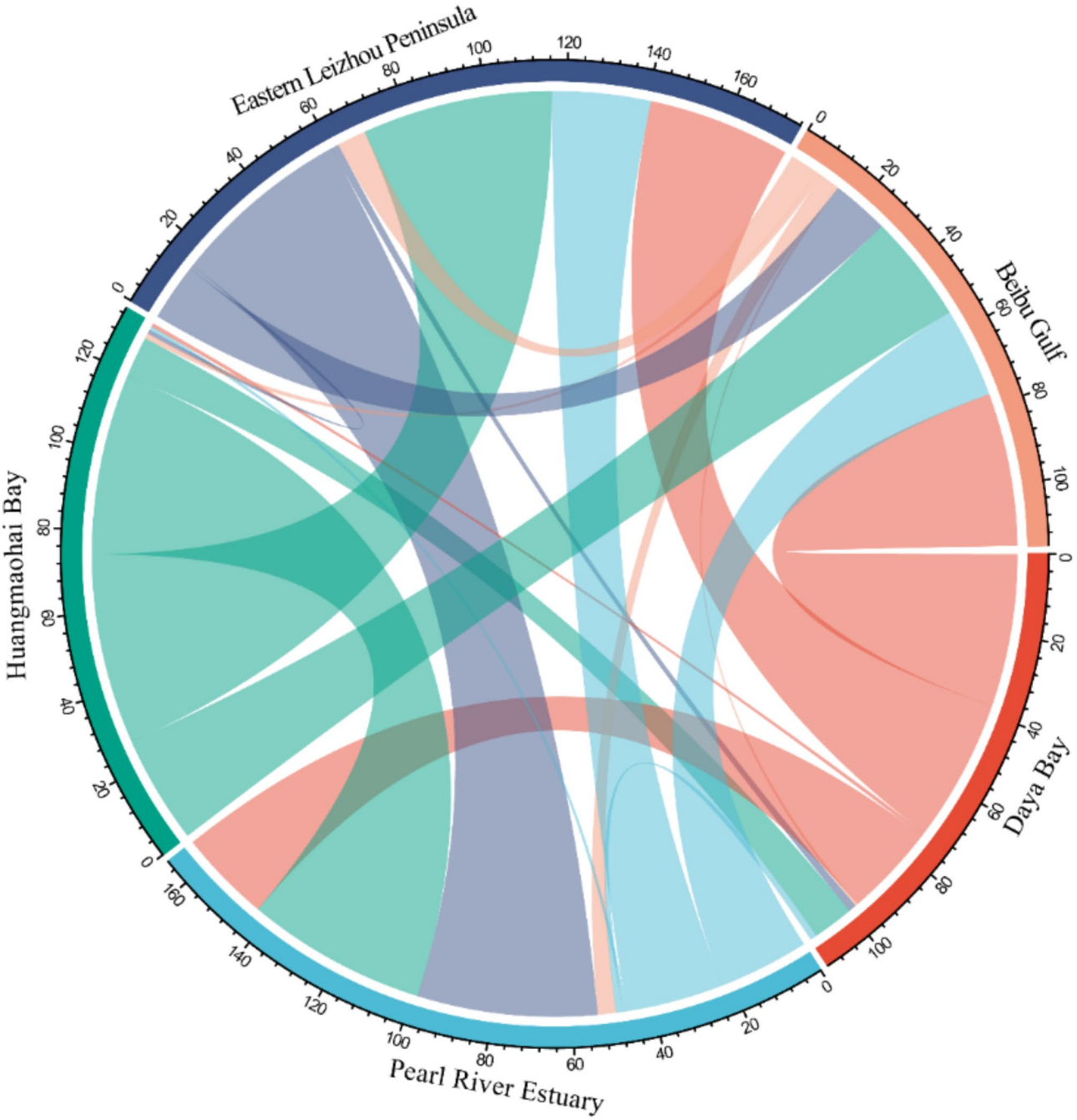


**Fig. 4**. Migration estimates were obtained using the maximum likelihood method implemented in MIGRATE-N 4.43. This analysis estimated recent migration rates and self-replenishment among five regions: Daya Bay, Pearl River Estuary, Huangmaohai Bay, the eastern Leizhou Peninsula, and Beibu Gulf, based on cytochrome oxidase subunit I (COI) sequences. Migration rates (M) were estimated using a Metropolis-Hastings MCMC approach, with a static mutation-scaled model. The analysis included four independent MCMC chains, each with 1,000,000 steps, a burn-in of 200,000 steps, and sampling every 100 iterations. Convergence was assessed using Gelman-Rubin diagnostics and effective sample size (ESS) values. The color of each line corresponds to the region of origin, representing gene flow from that specific area. The thickness of the lines reflects the magnitude of migration rates (M), while numerical values indicate the estimated migration rates (M) between regions.

portion, known as the northern South China Sea (NSCS), lies mainly within the subtropical zone and forms the first step of the SCS's three-tiered continental shelf. It is bordered by mainland China, the Indo-China Peninsula, Luzon Island, and Taiwan Island. The Beibu Gulf, partially enclosed gulf whose area is about 128,000 square kilometers, extends naturally to the west of the region. The NSCS links to the East China Sea (ECS) through the Taiwan Strait and connects to the western Pacific via the Luzon Strait[41,42].

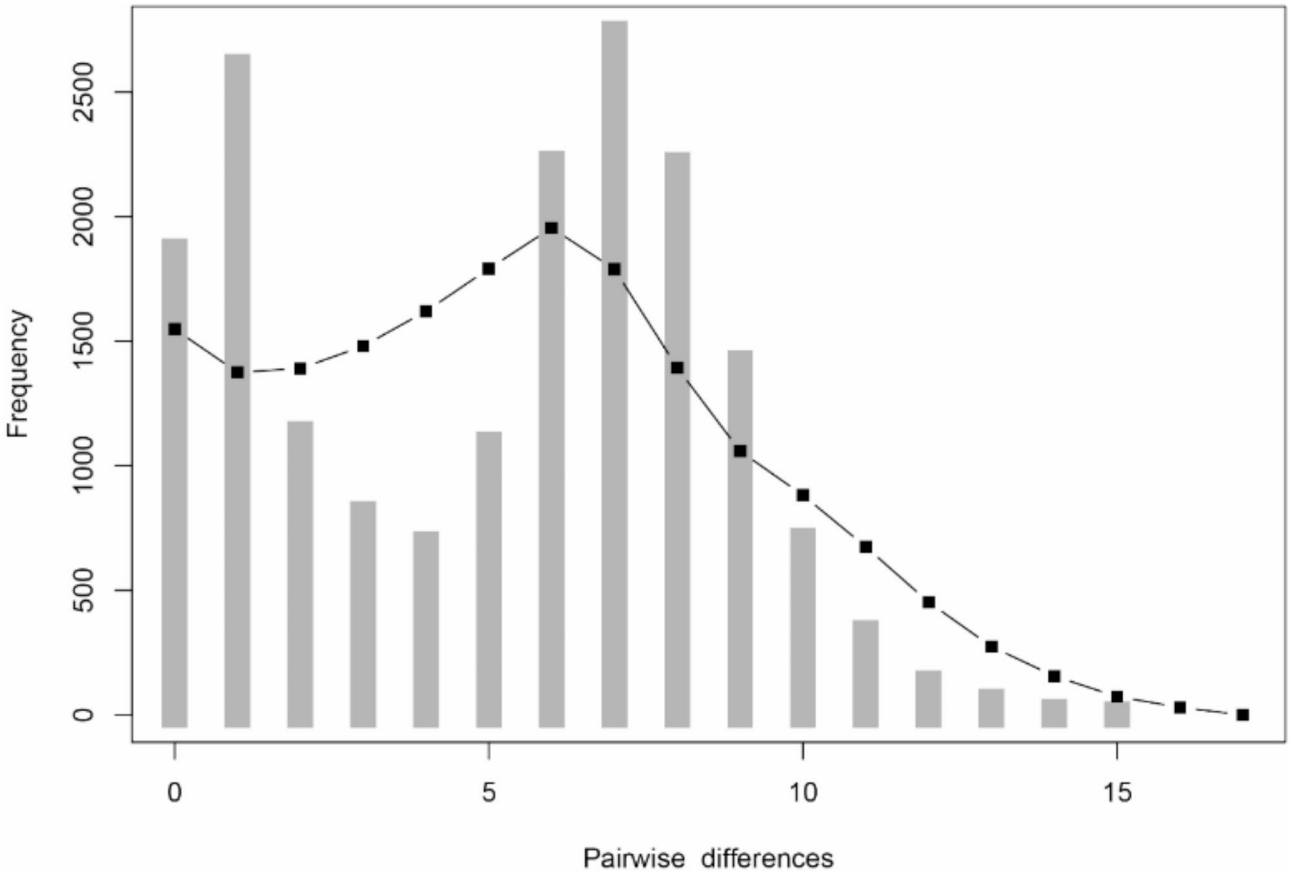


**Fig. 5**. Expected mismatch distributions under sudden expansion model (line) and observed mismatch distributions (bars) of COI for *Saccostrea echinata* from the northern South China Sea and the Beibu Gulf.

## Sample collection

In the northern South China Sea (NSCS), 5 sampling regions including 11 sampling sites were established in the rocky intertidal zones extending from Daya Bay to Hainan Island, specifically located at Daya Bay (S1, S2), Pearl River Estuary (S3, S4), Huangmaohai Bay (S5, S6), eastern regions of Leizhou Peninsula (S7, S11), and Beibu Gulf (S8, S9, S10). During the dry season (November to February of the following year), populations of *S. echinata* (the black-lip oyster) were collected (Fig. 1). Spatial coordinates (latitude and longitude) were recorded during the field surveys, and 10–24 samples were obtained from each site for morphological identification and subsequent DNA analysis. The adductor muscle tissue from each oyster was subsequently removed and stored at -20 °C.

## DNA extraction, PCR amplification, and sequencing

Genomic DNA was extracted from the adductor muscle tissue of specimens preserved at -20°C using the TIANamp Marine Animals DNA Kit (TIANGEN, China). In accordance with the manufacturer's protocol, the DNA concentration of each sample was measured using a NanoDrop ND-1000 UV-Vis Spectrophotometer (NanoDrop Technologies, USA). DNA samples with A260/A280 ratios between 1.8 and 2.0 were chosen as templates for PCR amplification. A fragment of the mitochondrial COI gene was amplified utilizing a pair of universal primers designed for broad taxonomic coverage CO1490F (5'-GGT CAA CAA ATC ATA AAG ATA TTG G-3') and CO2198R (5'-TAA ACT TCA GGG TGA CCA AAA AAT CA-3')[43].

The PCR reaction was carried out in a total volume of 20 µL, which included 2 µL of 10× PCR buffer, 0.2 µL of each primer at 25 µM, 0.8 µL of dNTPs at 10 µM, 2 µL of DNA template, 0.2 µL of Taq DNA polymerase supplied by Takara Bio Inc., and 14.6 µL of distilled water. The amplification protocol involved an initial denaturation at 95 °C for 3 min, succeeded by 35 cycles consisting of denaturation at 95 °C for 45 s, annealing at 55 °C for 60 s, and extension at 72 °C for 2 min. The process ended with a terminal extension at 72 °C for 3 min. The reactions were carried out utilizing an Applied Biosystems 2720 Thermal Cycler from the United States. All selected PCR products were further processed for bidirectional sequencing on an ABI 3730XL sequencer.

## Genetic analysis

The sequences underwent preliminary processing for visualization and assembly within BioEdit, after which they were automatically aligned utilizing the default settings[44]. For uniformity, we excluded the first 20 and last 10 base pairs from incomplete sequences. Post-alignment, ambiguous regions were trimmed. Genetic diversity

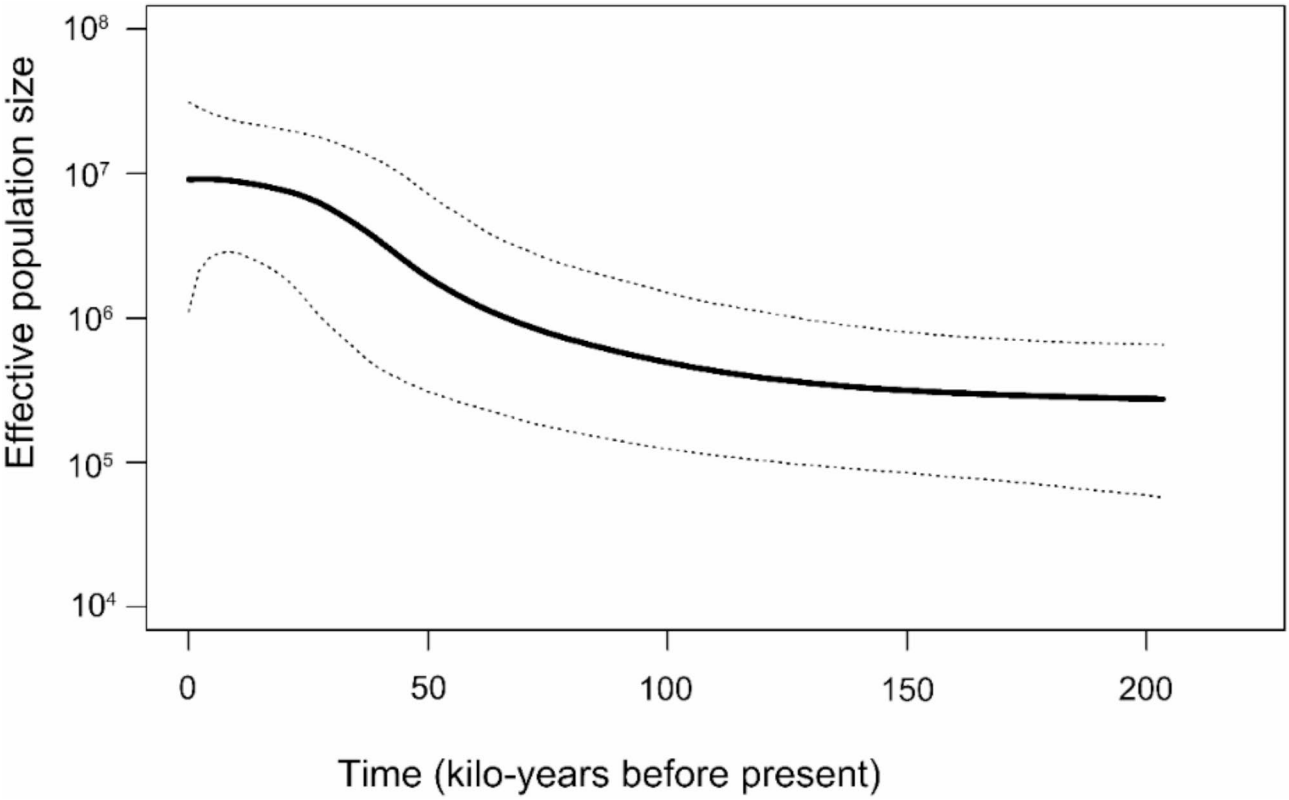


**Fig. 6**. The demographic trends of *Saccostrea echinata* in the northern South China Sea and the Beibu Gulf are depicted through a Bayesian skyline plot. The dark solid line represents the median estimate based on the assumption of a per site mutate at a rate of 2% per million years, with the dashed lines indicating the 95% highest posterior density (HPD) limits.

metrics for the COI sequences, such as the number of haplotypes (H), polymorphic sites (S), haplotype diversity (Hd), and nucleotide diversity ($\pi$), were determined using DnaSP version 5.0 [45].

To graphically illustrate the relationships among mtDNA haplotypes for each *S. echinata* individual, a haplotype network was built utilizing Haploviewer[46]. This software converts traditional phylogenetic trees (maximum likelihood tree and Bayesian inference tree) into haplotype genealogies, thereby facilitating the analysis of genetic relationships. The phylogenetic tree was built using the maximum likelihood method in PhyML 3.0, employing the GTR substitution model incorporating four distinct categories of gamma-distributed rate variations[47]. The GTR model is one of the most flexible and widely used models in phylogenetic analysis because it allows for unequal rates of substitution among all nucleotide pairs. To evaluate the degree of seascape genetic structure in *S. echinata*, the molecular differentiation among sites was determined systematically utilizing mitochondrial DNA markers ($\Phi_{ST}$, based on the infinite allele model) and carried out an Analysis of Molecular Variance (AMOVA) to explore the intricate distribution and patterns of genetic variation. Both analysis were performed using Arlequin version 3.5 [48]. Genetic differentiation was assessed by the AMOVA at three hierarchical levels, which included the regional level (Daya Bay, Pearl River Estuary, Huangmaohai Bay, eastern areas of Leizhou Peninsula, and Beibu Gulf), within each region among populations and within specific populations.

Principal coordinate analysis (PCoA), utilized linearized pairwise ΦST values (as $\Phi_{ST}$ /(1−$\Phi_{ST}$)), was employed to assess geographical variability in genetic structure as described by Slatkin[49]. This approach was used to evaluate differences in population genetic structure among regions in the northern South China Sea (NSCS). The 'cmdscale' function, sourced from the 'vegan' package was employed to conduct PCoA within the R statistical environment (https://www.r-project.org)[50]. To estimate effective population sizes and migration rates among regions in the NSCS, we used MIGRATE-N 4.43. We ran 4 independent Markov Chain Monte Carlo (MCMC) chains, each with 1,000,000 iterations, discarding the first 200,000 iterations as burn-in. Parameters were sampled every 100 iterations. The migration rates between populations were allowed to vary, and both migration rates and population sizes were treated as parameters to be estimated. Divergence times were estimated from the data without prior constraints. Convergence was assessed using the Gelman-Rubin diagnostic, which was < 1.1 for all parameters, indicating adequate convergence. The effective sample size (ESS) for migration rates was > 2000, indicating good mixing of the chains. The final migration rate estimates were reported with 95% credible intervals[51,52]. The computed parameters were subsequently presented as $P_{ij} = \theta_i M_{ij}$, where $P_{ij}$ denotes the effective number of migrants from population i to population j, $M_{ij}$ is determined by $m_{ij}/\mu$ ($m_{ij}$, indicating

the immigration rate from population i to population j, and μ, the mutation rate per generation), θ represents the size of the population adjusted by the mutation rate[51,52].

### Inferring the demographic history

To evaluate population demographic changes in *S. echinata*, such as expansions or bottlenecks, the analysis of Tajima's D and Fu's Fs statistics was conducted with Arlequin 3.5 [48,53,54]. To investigate whether the data for *S. echinata* in the northern South China Sea (NSCS) matched the results anticipated by the neutral theory framework, potentially pointing to a population bottleneck or expansion, this analysis utilized 10,000 permutations. According to neutral markers, negative Tajima's D and Fu's Fs values may be suggestive of a population expansion event. We then assessed the smoothness of the haplotype mismatch distribution analysis conducted with a sudden expansion model[55]. To evaluate the fit between the observed and expected mismatch distributions under the sudden expansion model, we conducted parametric bootstrapping with 1000 replicates using Arlequin 3.5. For this assessment, we employed the level of unevenness alongside the cumulative squared deviations[56].

The timeframe associated with the population expansion for *S. echinata* in the northern South China Sea (NSCS) was additionally estimated. The analysis of the mismatch distribution using the τ (tau) statistic formed part of this process, with the τ value subsequently translated into actual time (t) in years through the equation $\tau = 2ut$[55]. In this context, u denotes the mutation rate of the sequence, calculated using the formula $u = 2\mu k$, where μ represents the per-generation mutation rate of the mitochondrial DNA gene, and k represents the total number of nucleotides within the sequence. We adopted a mutation rate of 2% per million years[17,36,57,58], were chosen for analysis of mtDNA. Furthermore, the demographic history of *S. echinata* was evaluated utilizing a Bayesian skyline plot (BSP) implemented in BEAST 1.8.0 [59].

## Data availability

Sequence data that support the findings of this study have been deposited in the GenBank and are accessible via accession numbers PQ782955 to PQ783036.

Received: 30 December 2024; Accepted: 3 March 2025
Published online: 10 March 2025

## References

1. Bradbury, I. R. & Snelgrove, P. V. R. Contrasting larval transport in demersal fish and benthic invertebrates: the roles of behaviour and advective processes in determining Spatial pattern. *Can. J. Fish. Aquat. Sci.* **58**, 811–823. https://doi.org/10.1139/cjfas-58-4-811 (2001).
2. Bernatchez, S. et al. Seascape genomics of Eastern oyster (Crassostrea virginica) along the Atlantic Coast of Canada. *Evol. Appl.* **12**, 587–609. https://doi.org/10.1111/eva.12741 (2018).
3. Haye, P. A. et al. Phylogeographic structure in benthic marine invertebrates of the Southeast Pacific Coast of Chile with differing dispersal potential. *PloS One* **9**, e88613. (2014).
4. Waples, R. S. Separating the wheat from the Chaff: patterns of genetic differentiation in high gene flow species. *J. Hered.* **89**, 438–450. https://doi.org/10.1093/jhered/89.5.438 (1998).
5. Baus, E., Darrock, D. J. & Bruford, M. W. Gene-flow patterns in Atlantic and mediterranean populations of the Lusitanian sea star. *Mol. Ecol.* **14**, 3373–3382. https://doi.org/10.1111/j.1365-294X.2005.02681.x (2005).
6. Suárez, D., Jiménez-García, A. P. & Emerson, E. BC. Dispersal ability and its consequences for population genetic differentiation and diversification. *Proc. R. Soc. B* **289**, 20220489. https://doi.org/10.1098/rspb.2022.0489 (2022).
7. López-Márquez, V. et al. Genetic connectivity of two marine gastropods in the mediterranean Sea: seascape genetics reveals species-specific oceanographic drivers of gene flow. *Mol. Ecol.* **30**, 4608–4629. https://doi.org/10.1111/mec.16080 (2021).
8. Friis, G. et al. Rapid diversification of grey mangroves driven by geographic isolation and extreme environmental conditions in the Arabian Peninsula. *Mol. Ecol.* https://doi.org/10.1111/mec.17260 (2024).
9. Adams, S. M., Lindmeier, J. B. & Duvernell, D. D. Microsatellite analysis of the phylogeography, pleistocene history and secondary contact hypotheses for the killifish. *Mol. Ecol.* **15**, 1109–1123. https://doi.org/10.1111/j.1365-294X.2006.02859.x (2006).
10. Hellberg, M. E. Gene flow and isolation among populations of marine animals. *Annu. Rev. Ecol. Evol. S.* **40**, 291–310. https://doi.org/10.1146/annurev.ecolsys.110308.120223 (2009).
11. Gilg, M. R. & Hilbish, T. J. The geography of marine larval dispersal: coupling genetics with fine-scale physical oceanography. *Ecology* **84**, 2989–2998 (2003).
12. Yasuda, N. et al. Gene flow of (L.) in relation to ocean currents revealed by microsatellite analysis. *Mol. Ecol.* **18**, 1574–1590. https://doi.org/10.1111/j.1365-294X.2009.04133.x (2009).
13. M, C. Z. Taxonomic and phylogenetic studies of the *Saccostrea oysters* on the coastal areas of China Master thesis, Institution of Oceanology. *Chin. Acad. Sci.* (2018).
14. Southgate, P. C. & Lee, P. S. Hatchery rearing of the tropical Blacklip oyster Saccostrea echinata (Quoy and Gaimard). *Aquaculture* **169**, 275–281. https://doi.org/10.1016/S0044-8486(98)00382-2 (1998).
15. Glude, J. B. The applicability of recent innovations to mollusc culture in the Western Pacific Islands. *Aquaculture* **39**, 29–43. https://doi.org/10.1016/0044-8486(84)90257-6 (1984).
16. Nowland, S. J., Silva, C. N. S., Southgate, P. C. & Strugnell, J. M. Mitochondrial and nuclear genetic analyses of the tropical black-lip rock oyster (Saccostrea echinata) reveals population subdivision and informs sustainable aquaculture development. *BMC Genom.* https://doi.org/10.1186/s12864-019-6052-z (2019).
17. Crandall, E. D., Sbrocco, E. J., DeBoer, T. S., Barber, P. H. & Carpenter, K. E. Expansion dating: calibrating molecular clocks in marine species from expansions onto the Sunda shelf following the last glacial maximum. *Mol. Biol. Evol.* **29**, 707–719. https://doi.org/10.1093/molbev/msr227 (2011).
18. Baratti, M., Goti, E. & Messana, G. High level of genetic differentiation in the marine isopod Sphaeroma terebrans (Crustacea Isopoda Sphaeromatidae) as inferred by mitochondrial DNA analysis. *J. Exp. Mar. Biol. Ecol.* **315**, 225–234. https://doi.org/10.1016/j.jembe.2004.09.020 (2005).
19. Pereira, A. N., Márquez, A., Marin, M. & Marin, Y. Genetic evidence of two stocks of the Whitemouth croaker *Micropogonias furnieri* in the Río de La Plata and oceanic front in Uruguay. *J. Fish. Biol.* **75**, 321–331. https://doi.org/10.1111/j.1095-8649.2009.02321.x (2009).

20. Luttikhuizen, P. C., Drent, J. & Baker, A. J. Disjunct distribution of highly diverged mitochondrial lineage clade and population subdivision in a marine bivalve with pelagic larval dispersal. *Mol. Ecol.* **12**, 2215–2229. https://doi.org/10.1046/j.1365-294X.2003.01872.x (2003).
21. Malcher, G. et al. First evaluation of the population genetics and aspects of the evolutionary history of the Amazonian Snook, Centropomus Irae, and its association with the Amazon plume. *Hydrobiologia* **850**, 2115–2125. https://doi.org/10.1007/s10750-023-05223-5 (2023).
22. Kenchington, E., Heino, M. & Nielsen, E. E. Managing marine genetic diversity: time for action? *ICES J. Mar. Sci.* **60**, 1172–1176. https://doi.org/10.1016/S1054-3139(03)00136-X (2003).
23. Ward, R. D., Woodwark, M. & Skibinski, D. O. F. A comparison of genetic diversity levels in marine, freshwater, and anadromous fishes. *J. Fish. Biol.* **44**, 213–232. https://doi.org/10.1111/j.1095-8649.1994.tb01200.x (1994).
24. Grant, W. & Bowen, B. Shallow population histories in deep evolutionary lineages of marine fishes: insights from sardines and anchovies and lessons for conservation. *J. Hered.* **89**, 415–426. https://doi.org/10.1093/jhered/89.5.415 (1998).
25. Sekino, M., Sato, S., Hong, J. S. & Li, Q. Contrasting pattern of mitochondrial population diversity between an estuarine bivalve, the Kumamoto oyster Crassostrea Sikamea, and the closely related Pacific oyster C. gigas. *Mar. Biol.* **159**, 2757–2776. https://doi.org/10.1007/s00227-012-2037-z (2012).
26. Nagashima, K., Sato, M., Kawamata, K., Nakamura, A. & Ohta, T. Genetic structure of Japanese scallop population in Hokkaido, analyzed by mitochondrial haplotype distribution. *Mar. Biotechnol.* **7**, 1–10. https://doi.org/10.1007/s10126-004-3046-9 (2005).
27. Jiang, S., Li, Z., Li, J., Xu, K. & Ye, Y. Analysis of genetic diversity and structure of eight populations of Nerita yoldii along the Coast of China based on mitochondrial COI gene. *Animals* **14** (5), 718. https://doi.org/10.3390/ani14050718 (2024).
28. Kim, W. J. et al. Mitochondrial DNA sequence analysis from multiple gene fragments reveals genetic heterogeneity of Crassostrea ariakensis in East Asia. *Genes Genom.* **36**, 611–624. https://doi.org/10.1007/s13258-014-0198-5 (2014).
29. Ni, G., Li, Q., Kong, L. & Zheng, X. Phylogeography of bivalve cyclina sinensis: testing the historical glaciations and Changjiang river outflow hypotheses in Northwestern Pacific. *PloS One.* **7**, e49487. https://doi.org/10.1371/journal.pone.0049487 (2012).
30. Hu, L., Zhang, Z., Wang, H. & Zhang, T. Molecular phylogeography and population history of Crassostrea Sikamea (Amemiya, 1928) based on mitochondrial DNA. *J. Exp. Mar. Biol. Ecol.* **503**, 23–30. https://doi.org/10.1016/j.jembe.2017.11.004 (2018).
31. Li, L. et al. Divergence and plasticity shape adaptive potential of the Pacific oyster. *Nat. Ecol. Evol.* **2**, 1751–1760. https://doi.org/10.1038/s41559-018-0668-2 (2018).
32. Ma, H., Li, L., Xiao, S., Zhang, Y. & Yu, Z. Microsatellite-based study of population genetics of Crassostrea hongkongensis in Southern China. *Aquacult. Rep.* **19**, 100591. https://doi.org/10.1016/j.aqrep.2021.100591 (2021).
33. Samantha, J. N., Wayne, A. O. C., Shane, S. P. & Paul, C. S. Monsoonally driven reproduction in the tropical Black-Lip rock oyster < i > saccostrea echinata (Quoy & Gaimard, 1835) in Northern Australia. *J. Shellfish Res.* **38**, 89–100. https://doi.org/10.2983/035.038.0109 (2019).
34. Bertram, D. F. & Strathmann, R. R. Effects of maternal and larval nutrition on growth and form of planktotrophic larvae. *Ecology* **79**, 315–327. https://doi.org/10.2307/176885 (1998).
35. Voris, H. K. Maps of pleistocene sea levels in Southeast Asia: shorelines, river systems and time durations. *J. Biogeogr.* **27**, 1153–1167. https://doi.org/10.1046/j.1365-2699.2000.00489.x (2000).
36. Reeb, C. A. & Avise, J. C. A genetic discontinuity in a continuously distributed species: mitochondrial DNA in the American oyster, Crassostrea virginica. *Genetics* **124**, 397–406. https://doi.org/10.1093/genetics/124.2.397 (1990).
37. Bert, T. M., McCarthy, K. J., Cruz-Lopez, H. & Bogdanowicz, S. Character discriminatory power, character-set congruence, and the classification of individuals from hybrid zones: an example using stone crabs (*Menippe*). *Evolution* **50**, 655–671. https://doi.org/10.1111/j.1558-5646.1996.tb03876.x (1996).
38. Paulay, G. Effects of late cenozoic sea-level fluctuations on the bivalve faunas of tropical oceanic Islands. *Paleobiology* **16**, 415–434. https://doi.org/10.1017/S0094837300010162 (1990).
39. Colson, I. & Hughes, R. N. Rapid recovery of genetic diversity of Dogwhelk (*Nucella Lapillus* L.) populations after local extinction and recolonization contradicts predictions from life-history characteristics. *Mol. Ecol.* **13**, 2223–2233. https://doi.org/10.1111/j.1365-294X.2004.02245.x (2004).
40. Robalo, J. I. et al. Are local extinctions and recolonizations continuing at the colder limits of marine fish distributions? *Halobatrachus didactylus* (Bloch & Schneider, 1801), a possible candidate. *Mar. Biol.* **160**, 2461–2467. https://doi.org/10.1007/s00227-013-2241-5 (2013).
41. Morton, B. & Blackmore, G. South China sea. *Mar. Pollut Bull.* **42**, 1236–1263. https://doi.org/10.1016/s0025-326x(01)00240-5 (2001).
42. Nan, F., He, Z., Zhou, H. & Wang, D. Three long-lived anticyclonic eddies in the Northern South China sea. *J. Geophys. Res.* https://doi.org/10.1029/2010JC006790 (2011).
43. Folmer, O., Black, M., Hoeh, W., Lutz, R. & Vrijenhoek, R. DNA primers for amplification of mitochondrial cytochrome C oxidase subunit I from diverse metazoan invertebrates. *Mol. Mar. Biol. Biotechnol.* **3**, 294–299 (1994).
44. Hall, T. A. BioEdit: a user-friendly biological sequence algnment editor and analysis program for Windows 95/98/NT. *Nucl. Acids. Symp. Ser.* **41**, 95–98 (1999).
45. Librado, P. & Rozas, J. DnaSP v5: a software for comprehensive analysis of DNA polymorphism data. *Bioinformatics* **25**, 1451–1452. https://doi.org/10.1093/bioinformatics/btp187 (2009).
46. Salzburger, W., Ewing, G. B. & Von Haeseler, A. The performance of phylogenetic algorithms in estimating haplotype genealogies with migration. *Mol. Ecol.* **20**, 1952–1963. https://doi.org/10.1111/j.1365-294X.2011.05066.x (2011).
47. Guindon, S. et al. New algorithms and methods to estimate maximum-likelihood phylogenies: assessing the performance of PhyML 3.0. *Syst. Biol.* **59**, 307–321. https://doi.org/10.1093/sysbio/syq010 (2010).
48. Excoffier, L. & Lischer, H. E. L. Arlequin suite ver 3.5: a new series of programs to perform population genetics analyses under Linux and windows. *Mol. Ecol. Resour.* **10**, 564–567. https://doi.org/10.1111/j.1755-0998.2010.02847.x (2010).
49. Slatkin, M. A measure of population subdivision based on microsatellite allele frequencies. *Genetics* **139**, 457–462. https://doi.org/10.1093/genetics/139.1.457 (1995).
50. vegan: Community Ecology Package. (2019).
51. Beerli, P. & Felsenstein, J. Maximum-likelihood Estimation of migration rates and effective population numbers in two populations using a coalescent approach. *Genetics* **152**, 763–773. https://doi.org/10.1093/genetics/152.2.763 (1999).
52. Beerli, P., Mashayekhi, S., Sadeghi, M., Khodaei, M. & Shaw, K. Population genetic inference with MIGRATE. *Curr. Protoc. Bioinf.* **68** (1). https://doi.org/10.1002/cpbi.87 (2019).
53. Tajima, F. Statistical method for testing the neutral mutation hypothesis by DNA polymorphism. *Genetics* **123**, 585–595. https://doi.org/10.1093/genetics/123.3.585 (1989).
54. Fu, Y. X. Statistical tests of neutrality of mutations against population growth, hitchhiking and background selection. *Genetics* **147**, 915–925. https://doi.org/10.1093/genetics/147.2.915 (1997).
55. Rogers, A. R. & Harpending, H. Population growth makes waves in the distribution of pairwise genetic differences. *Mol. Biol. Evol.* **9**, 552–569. https://doi.org/10.1093/oxfordjournals.molbev.a040727 (1992).
56. Excoffier, L. Patterns of DNA sequence diversity and genetic structure after a range expansion: lessons from the infinite-island model. *Mol. Ecol.* **13**, 853–864. https://doi.org/10.1046/j.1365-294X.2003.02004.x (2004).
57. Loeza-Quintana, T. et al. Recalibrating the molecular clock for Arctic marine invertebrates based on DNA barcodes. *Genome* **62**, 200–216. https://doi.org/10.1139/gen-2018-0107 (2019).

58. Li, J., Foighil, Ó., Park, J. K. & D. & Triton's Trident: cryptic neogene divergences in a marine clam (Lasaea australis) correspond to Australia's three temperate biogeographic provinces. *Mol. Ecol.* **22**, 1933–1946. https://doi.org/10.1111/mec.12220 (2013).
59. Drummond, A. J. & Rambaut, A. B. E. A. S. T. Bayesian evolutionary analysis by sampling trees. *BMC Evol. Biol.* **7**, 214. https://doi.org/10.1186/1471-2148-7-214 (2007).

## Acknowledgements
We would like to express our sincere gratitude to all our colleagues and students who assisted with the sampling process. We are also deeply grateful to Dr. Jian Liao from Guangdong Ocean University for his invaluable help with the data analysis. Their contributions have been instrumental to the success of this project.

## Author contributions
Yafang Li conceptualized the study, developed the methodology, curated the data, and wrote the original draft. Lianggen Wang contributed to software development and created visualizations. Yingmin Wang conducted investigations, prepared samples, and carried out experiments. Quehui Tang performed formal analysis, created visualizations, and contributed to software and methodology. Shuangshuang Liu participated in the investigation. Jiajia Ning and Delian Huang reviewed and edited the manuscript. Lei Xu supervised the project, contributed to the methodology, and also reviewed and edited the manuscript. Feiyan Du supervised the study, conceptualized the research, developed software, and secured funding. All authors reviewed the manuscript. Funding information This study was supported by the Hainan Provincial Natural Science Foundation of China [323QN333], [324MS131], [422MS156], the foundation of Guangdong Provincial Observation and Research Station for Coastal Upwelling Ecosystem [CUE202305] and Guangdong Provincial Environmental Protection Special Fund [PM-zx555-202206-253].

## Funding
This study was supported by the Hainan Provincial Natural Science Foundation of China [323QN333], [324MS131], [422MS156], the foundation of Guangdong Provincial Observation and Research Station for Coastal Upwelling Ecosystem [CUE202305] and Guangdong Provincial Environmental Protection Special Fund [PM-zx555-202206-253].

## Declarations

## Competing interests
The authors declare no competing interests.

## Additional information
**Supplementary Information** The online version contains supplementary material available at https://doi.org/10.1038/s41598-025-92747-6.

**Correspondence** and requests for materials should be addressed to L.X. or F.D.

**Reprints and permissions information** is available at www.nature.com/reprints.

**Publisher's note** Springer Nature remains neutral with regard to jurisdictional claims in published maps and institutional affiliations.